A Monte Carlo study of the anisotropic Heisenberg chain with spin 1

1986 J. Phys. A: Math. Gen. 19 493

(http://iopscience.iop.org/0305-4470/19/4/011)

J. Phys. A: Math. Gen. 19 (1986) 493-502. Printed in Great Britain

A Monte Carlo study of the anisotropic Heisenberg chain with spin 1

K Sogo† and M Uchinami‡

† Institute for Nuclear Study, University of Tokyo, Tanashi, Tokyo 188, Japan
‡ Laboratory of Mathematics, Meiji College of Pharmacy, Nozawa, Tokyo 154, Japan

Received 17 June 1985

Abstract. A Monte Carlo method for quantum spin-1 systems is presented. The internal energy and longitudinal correlation functions are computed in the antiferromagnetic region. Some exponents and the phase diagram are derived with good accuracy.

1. Introduction

Recently the one-dimensional anisotropic Heisenberg model with spin 1 has attracted much attention, both theoretical and experimental. In particular, Haldane (1983a, b) proposed a conjecture that this model (more generally, systems with integral spin) has a quite different phase diagram compared with the spin-$\frac{1}{2}$ case.

Stimulated by this conjecture, many numerical studies have been done. Botet and Jullien (1983, 1984) and Botet *et al* (1984) solved finite size ($N = 2$-12) systems numerically. Their analysis by the finite-size scaling hypothesis seems, they claim, to support Haldane's conjecture. The work of Bonner and Müller (1984) shows, however, a doubt about the procedure of finite size scaling; even for the spin-$\frac{1}{2}$ (exactly solvable) case it gives a wrong answer. Other numerical works (Glans and Schneider 1984, Sólyom and Ziman 1984) give slightly different phase diagrams.

One of the authors (KS) solved (Sogo 1984), on the other hand, the completely integrable XXZ model with arbitrary spin S, and found that there is no qualitative difference between the cases of integral and half-integral spins in the excitation spectrum. If the universality class of this XXZ model is large enough to cover the ordinary Heisenberg model, Haldane's conjecture is to be negated.

In such a way, the issue whether the excitation is massive or massless has not been settled yet even for the isotropic case. In the present paper we consider this problem by a Monte Carlo (MC) method.

The MC simulations enable us to treat large systems ($N = 40$ in this work) easily. The MC procedure for quantum systems was first proposed by Suzuki in 1976. Recently the procedure of Hirsch *et al* (1982) was applied and extended by Nakamura *et al* (1985) to study the anisotropic Heisenberg model with spin $\frac{1}{2}$ (including the dimerised case). We found that the simulations reproduce the exact theory with good accuracy.

In § 2, the MC procedure used in Nakamura *et al* (1985) is generalised to higher spins. The results of simulations are summarised in § 3, and they show that Haldane's conjecture does not hold in the spin-1 case. Section 4 is devoted to conclusions and discussions.

0305-4470/86/040493+10$02.50

2. Monte Carlo procedure

The Hamiltonian considered in this paper is

$$H = \sum_{n=1}^{N} [-J(S_n^x S_{n+1}^x + S_n^y S_{n+1}^y) + J_3 S_n^z S_{n+1}^z + D(S_n^z)^2], \tag{1}$$

where the S_n^α ($\alpha = x, y, z$) are spin operators of magnitude 1. Although the sign of the first term is changed for later convenience, it does not affect the physical arguments, because the unitary transformation $U = \exp(\mathrm{i}\pi \Sigma_{\mathrm{odd}} S_n^z)$ changes this sign.

The statistical mechanical object we consider is the canonical ensemble, or the partition function

$$Z = \mathrm{Tr}(\mathrm{e}^{-\beta H}). \tag{2}$$

Although our case of spin 1 cannot be interpreted as a fermion problem like the spin-$\frac{1}{2}$ case (Hirsch *et al* 1982), we can expect that the checkerboard arrangement still works very well. Namely we decompose the Hamiltonian into two parts $H = H_1 + H_2$, and using the Trotter formula we put them on a checkerboard. We have

$$Z \simeq \mathrm{Tr}(V_1 V_2)^L, \tag{3}$$

$$V_{1(2)} = \prod_{n:\,\mathrm{odd\,(even)}} \exp(-\Delta\tau H_{n,n+1}),$$

where $\Delta\tau = \beta/L$ and

$$H_{n,n+1} = -J(S_n^x S_{n+1}^x + S_n^y S_{n+1}^y) + J_z S_n^z S_{n+1}^z + \tfrac{1}{2}D[(S_n^z)^2 + (S_{n+1}^z)^2].$$

The local transition matrix $V = \exp(-\Delta\tau H_{n,n+1})$ is a 9×9 matrix, given by (in the z-component diagonal representation)

$$V = \begin{pmatrix} D_s & 0 & 0 & 0 & 0 & 0 & 0 & 0 & 0 \\ 0 & S_1 & 0 & R_1 & 0 & 0 & 0 & 0 & 0 \\ 0 & 0 & S & 0 & R & 0 & A & 0 & 0 \\ 0 & R_1 & 0 & S_1 & 0 & 0 & 0 & 0 & 0 \\ 0 & 0 & R & 0 & T & 0 & R & 0 & 0 \\ 0 & 0 & 0 & 0 & 0 & S_1 & 0 & R_1 & 0 \\ 0 & 0 & A & 0 & R & 0 & S & 0 & 0 \\ 0 & 0 & 0 & 0 & 0 & R_1 & 0 & S_1 & 0 \\ 0 & 0 & 0 & 0 & 0 & 0 & 0 & 0 & D_s \end{pmatrix} \tag{4}$$

where we have introduced

$$\begin{aligned} D_s &= \exp[-\Delta\tau\,(D + J_z)], \\ S_1 &= \cosh(\Delta\tau J)\exp(-\Delta\tau D/2), \\ R_1 &= \sinh(\Delta\tau J)\exp(-\Delta\tau D/2), \\ S &= u_1^2\,\mathrm{e}^{\lambda_+} + \tfrac{1}{2}\mathrm{e}^{\lambda_0} + v_1^2\,\mathrm{e}^{\lambda_-}, \\ A &= u_1^2\,\mathrm{e}^{\lambda_+} - \tfrac{1}{2}\mathrm{e}^{\lambda_0} + v_1^2\,\mathrm{e}^{\lambda_-}, \\ T &= u_2^2\,\mathrm{e}^{\lambda_+} + v_2^2\,\mathrm{e}^{\lambda_-}, \\ R &= u_1 u_2\,\mathrm{e}^{\lambda_+} + v_1 v_2\,\mathrm{e}^{\lambda_-}. \end{aligned} \tag{5}$$

In the expression (5), we put

$$\lambda_{\pm} = -\Delta\tau\tfrac{1}{2}\{D - J_z \pm [(D - J_z)^2 + 8J^2]^{1/2}\},$$

$$\lambda_0 = -\Delta\tau(D - J_z),$$

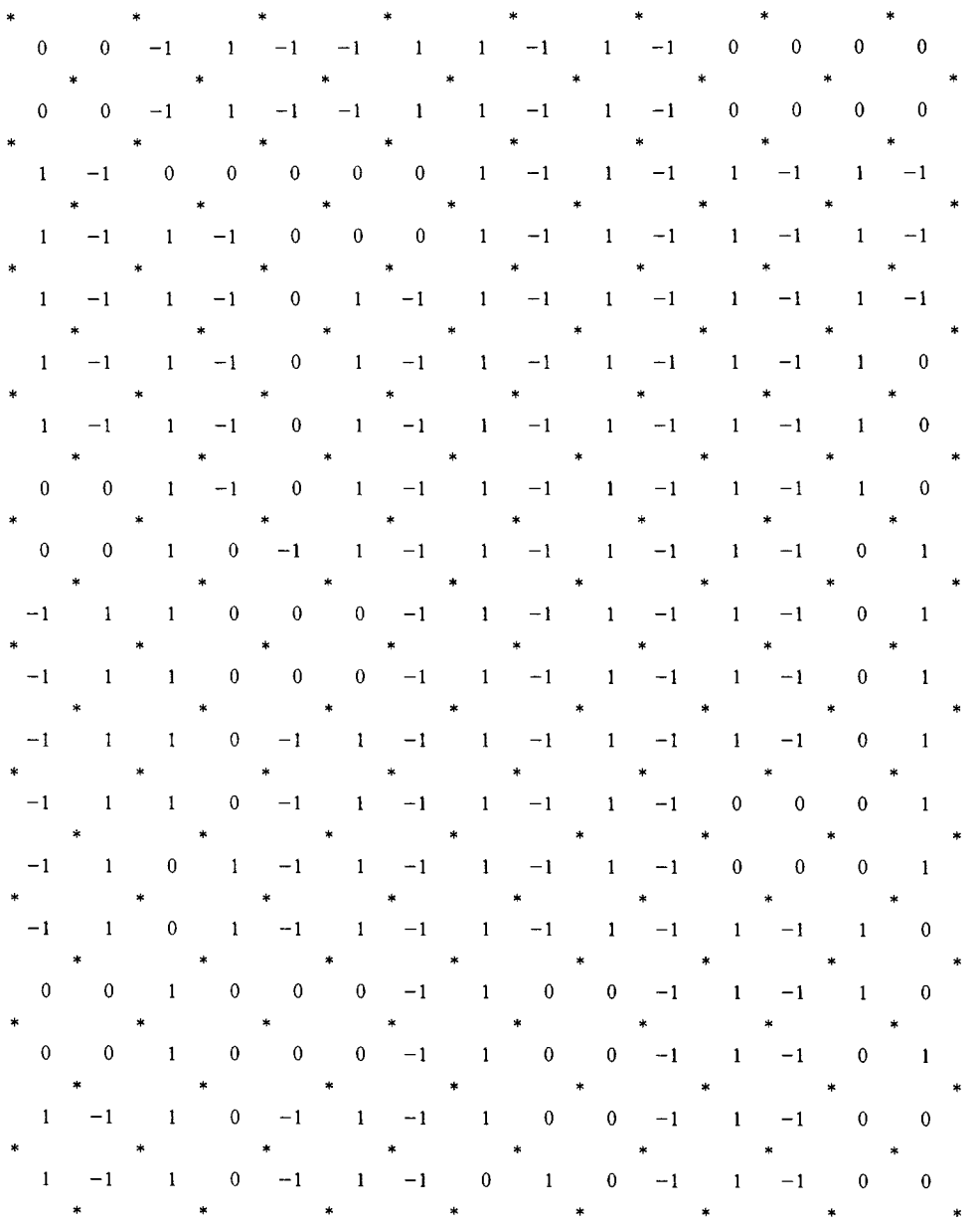

Figure 1. A part of a typical configuration for the case $J = J_z = 2.0$, $D = 0.0$. In this checkerboard pattern, each * part represents the interaction V. The number at each corner of a * is the value of the spin. The horizontal direction points to the spatial lattice, and the vertical one points to the imaginary-time axis.

$$u_1 = J/[2J^2 + (\lambda_-/\Delta\tau)^2]^{1/2}, \qquad u_2 = u_1\lambda_-/(J\Delta\tau),$$
$$v_1 = J/[2J^2 + (\lambda_+/\Delta\tau)^2]^{1/2}, \qquad v_2 = v_1\lambda_+/(J\Delta\tau).$$

It should be noted that $D_s \sim R$ are all positive definite.

Since the Hamiltonian (1) conserves the z component S^z of total spins, the Hilbert space is decomposed according to $S^z = N, \ldots, -N$. Because we are interested in the antiferromagnetic case ($J_z \geqslant 0$), we restrict our consideration to the subspace of $S^z = 0$ in this paper.

Now the MC simulation can be performed by a heat bath algorithm based on the transition probability derived from matrix (4). In figure 1 we show a typical configuration for the case of $J = J_z = 2.0$, $D = 0.0$ and $\Delta\tau = 0.2$. Throughout this paper the results are obtained from the MC data of 10 000 MC sweeps after 5000 sweeps of thermalisation. The measurements on 10 000 samples are divided into 200 sets of 50 samples, and the usual calculation of the average and standard deviation is applied to them. The size of system simulated is $N = 40$, and the value of L is kept to 30 for the most part. Correspondingly the relative temperature is $T/J = \frac{1}{12} = 0.083$, which can be regarded as sufficiently low.

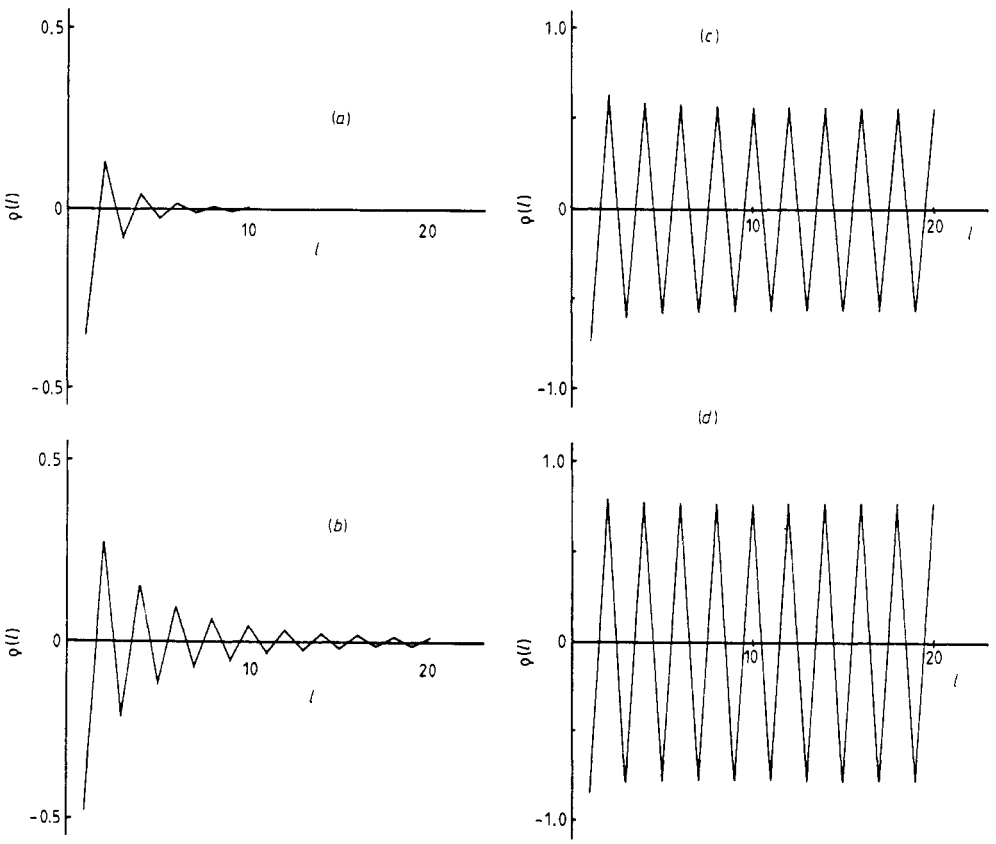

Figure 2. Longitudinal correlation fucntion of ordinary Heisenberg model ($D = 0$) for (a) $\Delta = 0.75$, (b) $\Delta = 1.0$, (c) $\Delta = 1.25$, (d) $\Delta = 1.5$ ($\Delta = J_z/J$).

3. Results of Monte Carlo simulations

3.1. Ordinary Heisenberg model ($D = 0$)

First let us discuss the case of the ordinary Heisenberg model. In figure 2 the correlation function $\rho(l) = \langle S_n^z S_{n+l}^z \rangle$ is shown for some $\Delta = J_z/J$. One can notice a qualitative difference between the behaviour for $\Delta > 1$ and $\Delta \leqslant 1$: we have a residual staggered magnetisation for $\Delta > 1$, while the correlation function for $\Delta \leqslant 1$ damps rapidly. We performed further simulations near $\Delta = 1$ to get the detailed information.

In figure 3 we show the staggered magnetisation M_s for various Δ in the region $\Delta > 1$. The curve obtained looks quite similar to the corresponding one for the spin-$\frac{1}{2}$ case, which is given in figure 4 for comparison. It should be noted that there is no

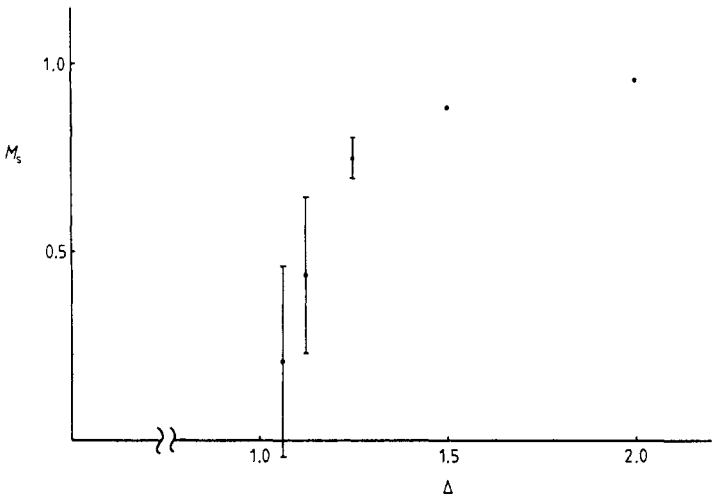

Figure 3. Staggered magnetisation M_s plotted against anisotropy $\Delta = J_z/J$.

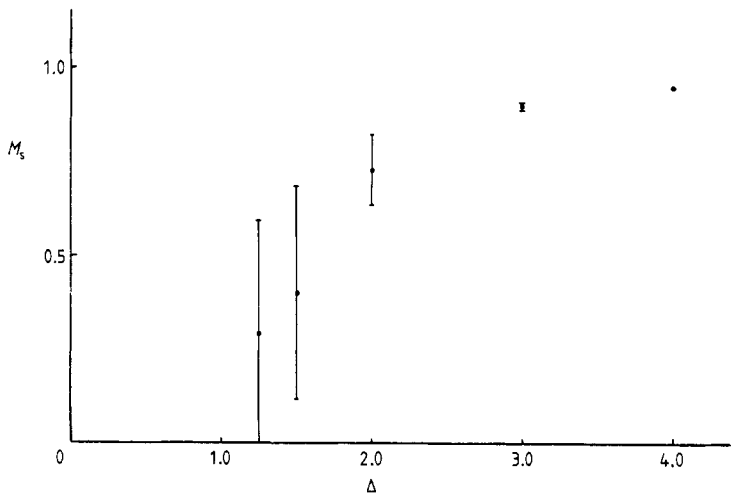

Figure 4. Staggered magnetisation M_s plotted against anisotropy $\Delta = J_z/J$ for $S = \frac{1}{2}$ (compare with figure 3).

indication of Haldane's phase near $\Delta = 1$. On the contrary, the behaviour near $\Delta = 1$ might be of essential singular type ($\sim \exp[-\text{constant}/(\Delta - 1)^{1/2}]$), which is the case for $S = \frac{1}{2}$. This behaviour is also expected in the exactly solvable XXZ model (Sogo 1984) for arbitrary spin S.

Now let us turn to the case of $\Delta \leqslant 1$. In figure 5 we give the exponent x estimated from the data for some values of Δ in the region $\Delta \leqslant 1$. In the above the least-squares fitting program (SALS) is used on the assumption that $\rho(l) \sim (-1)^l l^{-x}$.

In our simulations the internal energy was measured along with the correlation function. In figure 6 is shown the internal energy for various Δ at the temperature

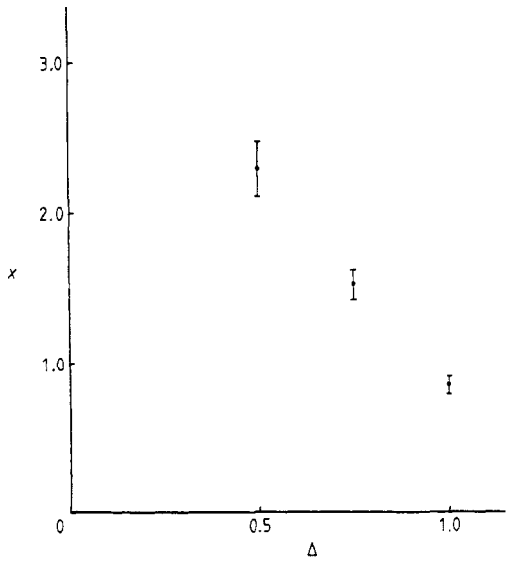

Figure 5. Exponent x of correlation function plotted against anisotropy $\Delta = J_z/J$.

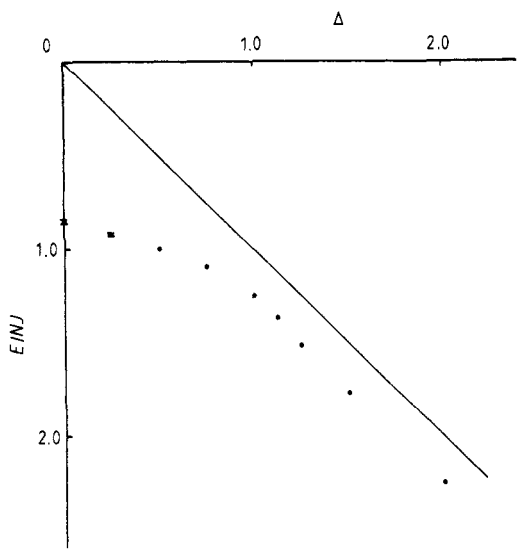

Figure 6. Internal energy at $T/J = 0.083$ plotted against anisotropy $\Delta = J_z/J$.

$T/J = 0.083$. The full line is $E/NJ = \Delta$, which is the expectation value for the Néel state. As is expected, the internal energy curve approaches the Néel line for large Δ asymptotically.

To close this subsection we show in figure 7 the change of the internal energy with temperature, from which we see that the specific heat (derivative of the internal energy) has a peak around $T/J \sim 1.0$.

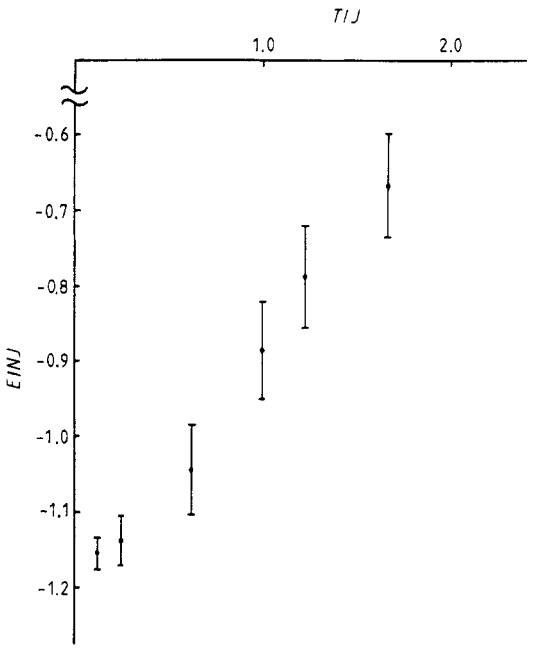

Figure 7. Internal energy of isotropic Heisenberg model ($\Delta = 1$, $D = 0$) plotted against temperature.

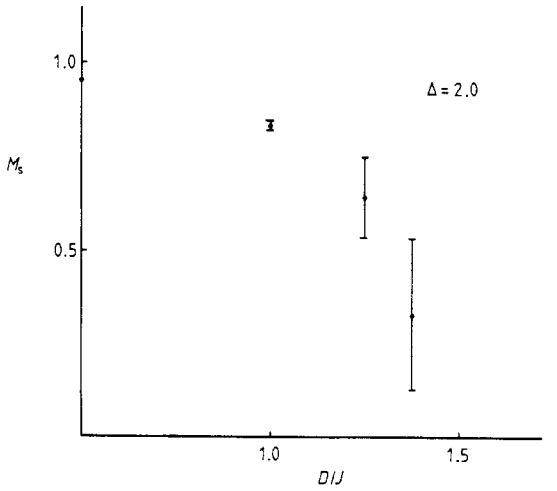

Figure 8. Staggered magnetisation M_s for $\Delta = 2.0$ against single ion anisotropy D.

3.2. *Effect of the single ion anisotropy* ($D \neq 0$)

Now let us discuss the case of $D \neq 0$. From a naive consideration we can expect that the value of D controls the behaviour of the residual staggered magnetisation in the correlation $\langle S_n^z S_{n+l}^z \rangle$: when D exceeds a critical value $D_c(\Delta)$, which depends on Δ, the staggered magnetisation vanishes. In general the staggered magnetisation behaves near critical D_c as $M_s \sim (D_c - D)^y$.

In figure 8 the magnetisation M_s is plotted against D for the case of $\Delta = 2.0$. The behaviour is just as we expected. In figure 9 we give the exponent y estimated from the data for some values of Δ.

Finally we can construct a phase diagram from the determined $D_c(\Delta)$. Figure 10 is the phase diagram obtained from our simulations. The right region is the phase with staggered magnetisation and gap, while the left region is gapless. The broken line in the figure represents a result of the mean field theory (Sólyan and Ziman 1984).

To confirm whether the transition between singlet and planar phases exists, as the mean field theory says, or not, the measurement of the transverse correlation function $\langle S_n^+ S_{n+l}^- \rangle$ is required. For this purpose some complicated calculations are needed, and will be studied in future work.

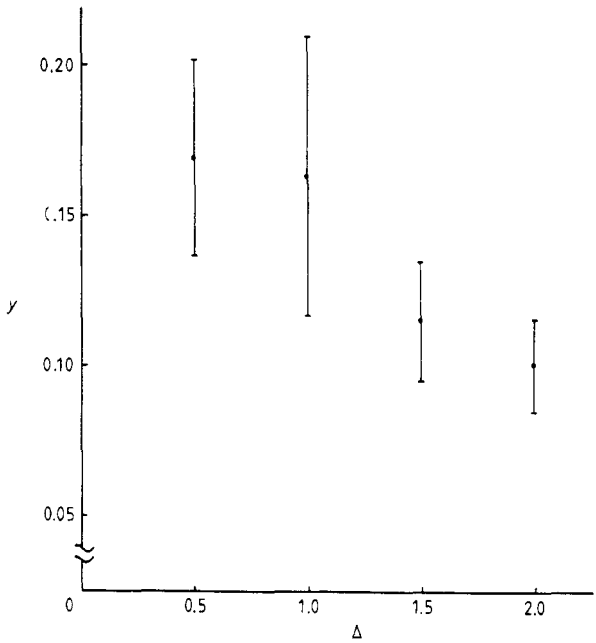

Figure 9. Exponent y of staggered magnetisation M_s, defined by $M_s \sim (D_c - D)^y$, for some values of Δ.

4. Conclusions and discussions

We performed Monte Carlo simulations of the anisotropic Heisenberg model with spin 1. The longitudinal correlation function and the internal energy are measured at various points in the antiferromagnetic region. From these data some exponents and the phase diagram are derived with good accuracy.

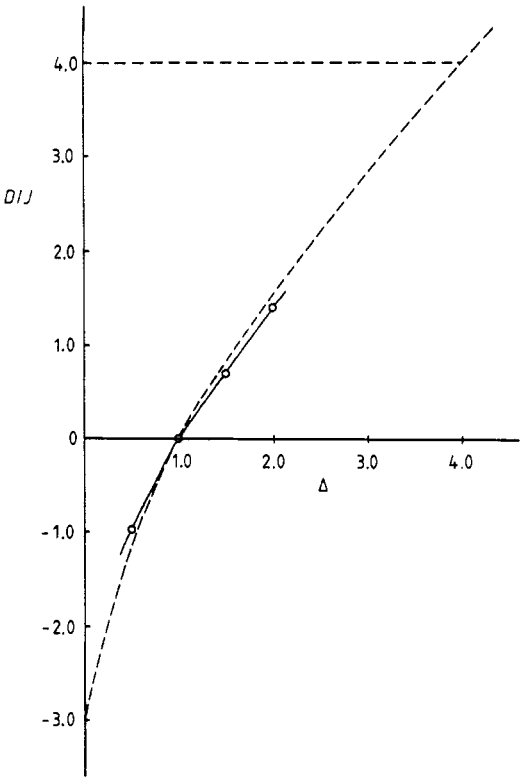

Figure 10. Phase diagram estimated from simulations. Open circles are the obtained critical $D_c(\Delta)$. The right side of the full line is the phase with staggered magnetisation and gap, and the left region is the gapless phase. The broken line is the result of the mean field theory. The line at $D/J = 4$ separates the planar and singlet phases.

One might suspect that there certainly exists a finite size effect. To check how large is this effect, we did simulations of the typical case $\Delta = 1.25$ and $D = 0$ for $N = 20$, 30 and 40. The result is given in figure 11, where the energy and correlation function $\rho(10)$ are shown as representative examples. The effect is rather small and is masked in the error of measurement for $N \geq 30$.

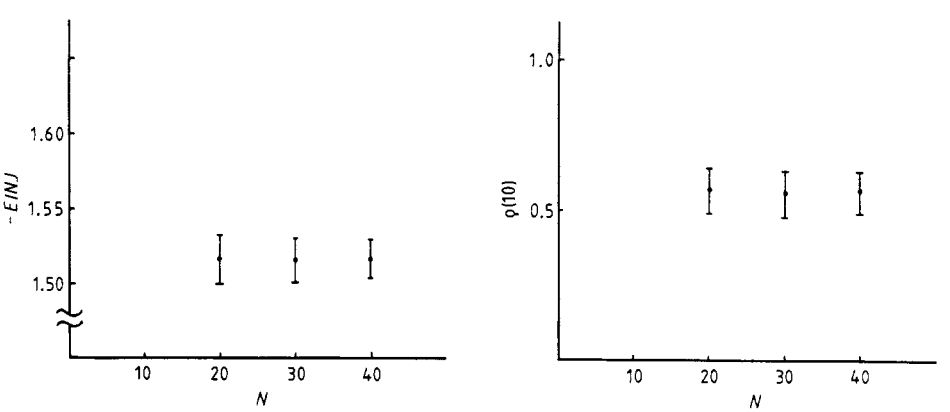

Figure 11. Finite size effect. Note that the size effect is very small for $N \geq 30$.

Although we did not focus on the relevance of our model to actual experiments, there should be some remarks on this point. Our model applies to the materials $CsNiCl_3$ and $RbNiCl_3$ ($\Delta = 1$, $D = 0$). For the full comparison with experiments, however, it is desirable to compute the dynamical form factors $S_{\alpha\beta}(q, \omega)$, which are the Fourier transforms of both longitudinal and transverse correlation functions.

Although there is no essential difficulty in computing static correlations on the simulations, we need a new idea to compute the dynamical ones, as was discussed in Hirsch *et al* (1982). Recent microcanonical and Langevin equation approaches might give a hint to this problem.

Acknowledgments

The authors are very grateful to Dr Atsushi Nakamura, who invited them to the world of Monte Carlo simulations. They also thank Professor Miki Wadati for his continuous encouragement. One of the authors (KS) benefited from discussions with the members of the theory division at INS. The numerical calculation was done by FACOM M-380 at the INS computer centre.

References

Bonner J C and Müller G 1984 *Phys. Rev.* B **29** 5216
Botet R and Jullien R 1983 *Phys. Rev.* B **27** 613
—— 1984 *Phys. Rev.* B **29** 5222
Botet R, Jullien R and Kolb M 1984 *Phys. Rev.* B **28** 3914
Glaus U and Schneider T 1984 *Phys. Rev.* B **30** 215
Haldane F D M 1983a *Phys. Lett.* **93A** 464
—— 1983b *Phys. Rev. Lett.* **50** 1153
Hirsch J E, Sugar R L, Scalapino D J and Blankenbecler R 1982 *Phys. Rev.* B **26** 5033
Nakamura A, Sogo K and Uchinami M 1985 *INS-Rep.* 533
Sogo K 1984 *Phys. Lett.* **104A** 51
Sólyom J and Ziman T A L 1984 *Phys. Rev.* B **30** 3980
Suzuki M 1976 *Prog. Theor. Phys.* **56** 1454